Doppler-based lateral motion tracking for optical coherence tomography

Nicolás Weiss,* Ton G. van Leeuwen, and Jeroen Kalkman

Biomedical Engineering & Physics, Academic Medical Center, University of Amsterdam, PO Box 22700, 1100 DE Amsterdam, the Netherlands

**Corresponding author: n.m.weiss@amc.uva.nl*

Received March 15, 2012; accepted April 16, 2012;
posted April 19, 2012 (Doc. ID 164900); published June 4, 2012

Nonuniform lateral scanning of the probe beam in optical coherence tomography produces imaging artifacts and leads to a morphologically inaccurate representation of the sample. Here, we demonstrate a solution to this problem, which is based on the Doppler shift carried by the complex-valued depth-resolved scattering amplitude. Furthermore, we demonstrate the feasibility of Doppler flow velocity measurements in underlying flow channels while laterally scanning the imaging probe over large surfaces with arbitrary and varying velocity. Finally, we performed centimeters-long hand-held B-mode imaging of skin *in vivo*. © 2012 Optical Society of America

OCIS codes: 170.3880, 170.4500, 170.3010, 330.4150.

Optical coherence tomography (OCT) is an imaging technique in which low coherence interferometry is used to produce depth-dependent backscatter profiles from tissue (A-lines). By lateral scanning the OCT beam or the tissue, high resolution cross-sectional images of tissue are obtained. As OCT systems generally operate at constant A-line rates, a uniform velocity sweep across the sample yields an ensemble of A-lines that are uniformly sampled in space, resulting in a morphologically correct image. In general, scanning of the OCT probe beam is performed with galvanometric scanners that can achieve high frequency, constant velocity sweeps, with large duty cycles. However, their lateral scan range is limited to several millimeters.

Manual scanning of the imaging probe has been proposed as an alternative method for lateral scanning. However, contrary to galvanometric scanning, in manual scanning OCT, A-lines are no longer sampled uniformly in space due to the nonuniform velocity. Yet, by determining the nonuniform relative displacement trajectory of the scanning probe, the raw OCT image can be spatially resampled to construct a morphologically accurate image of the sample. In [1], the relative displacement is determined based on the correlation of adjacent A-lines. Consequently, this approach relies on *a priori* knowledge of the sample structure and its scattering properties. In [2,] the relative displacement is measured with an external optical monitoring system that consists of a tracking camera and identification markers attached to the imaging probe to track its position during image acquisition. While this approach allows for a complete estimation of the position and orientation of the imaging probe, its main drawback is that the OCT system becomes more complex and expensive, and dependent on a direct line of sight between the monitoring camera and the OCT probe.

Here, we propose to estimate the relative displacement based on the intrinsic OCT signal. Assuming a solid sample with stationary scatterers, the Doppler shift, measured at depth z and time t, quantifies the velocity of the moving probe over a sample. The probe velocity is approximated by [3]

$$v(z,t,t+T)=\frac{\lambda_c}{4\pi n\cos\theta}\frac{\arg[a_{\mathrm{OCT}}(z,t)a^*_{\mathrm{OCT}}(z,t+T)]}{T}, \quad (1)$$

where λ_c is the center wavelength of the source, n is the refractive index of the sample, θ is the angle between the optical axis of the probe and the direction of motion, T is the time period between two adjacent A-lines, and $a_{\mathrm{OCT}}(z,t)$ is the complex-valued depth-resolved scattering amplitude. The one-dimensional displacement trajectory of the probe is calculated by numerically integrating (1). Then, the ensemble of A-lines defined by $|a_{\mathrm{OCT}}(z,t)|$ is resampled from a uniform time axis to a uniform displacement axis, thus correcting for the image distortion caused by the nonuniform lateral scan velocity. We assume that the velocity measurements $v(z,t,t+T)$ are uncorrelated random variables with identical standard deviations, a linear interpolation of (1), and a shot noise limited detection. Then, the minimum displacement error is written as [3]

$$\Delta x(t+T)=\frac{\lambda_c}{2\sqrt{2}\pi n\cos\theta}\sqrt{N}\Delta\phi, \quad (2)$$

with N the number of A-lines acquired during time $t+T$, and $\Delta\phi$ the phase stability of the OCT system.

We implemented the displacement estimation technique in a home-built spectral-domain OCT system operating at a center wavelength $\lambda_c = 1300$ nm and an A-line acquisition rate $f_A = 16.846$ KHz [4]. To illustrate the effects of nonuniform scanning, we performed OCT imaging of a silicon-based tissue phantom with a constant pitch ridge pattern [5] that was placed on a motorized translation stage (Zaber T-LS28-M) and was programmed to move with uniform and nonuniform velocities. The velocity was measured at a depth of 250 μm beneath the surface of the tissue phantom. For all measurements the angle θ in (1) is calibrated by translating the stage a known distance and equating the calculated and programmed distances.

Figure 1(a) shows a morphologically correct OCT image of the tissue phantom acquired by translating the stage with quasi-uniform velocity. Figure 1(b) shows the same tissue phantom measured with a nonuniform

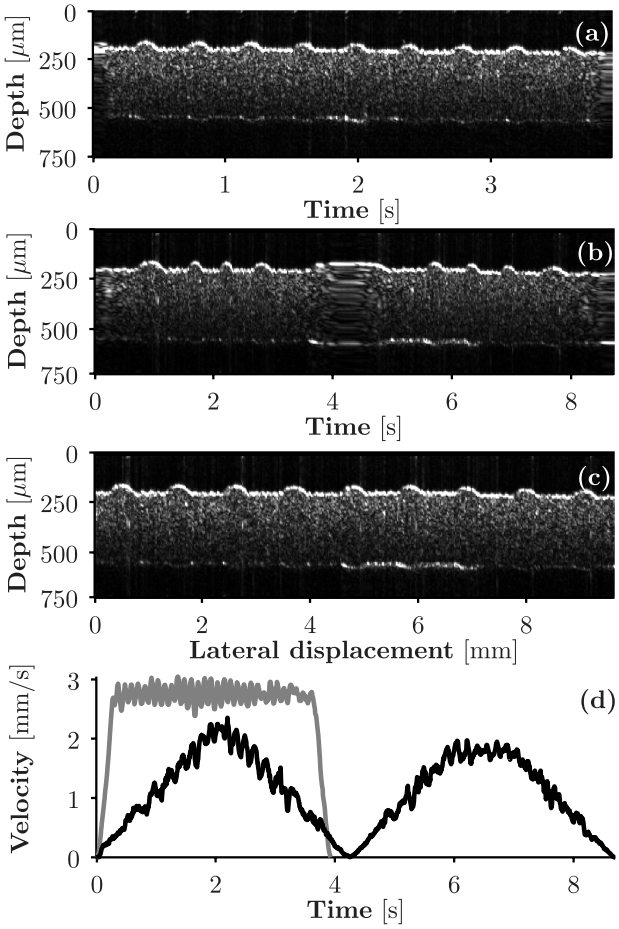

Fig. 1. Doppler-based lateral motion tracking of a tissue phantom. (a) Quasi-uniform motion and control image. (b) Nonuniform motion plotted in a uniform time axis showing lateral motion artifacts. (c) Nonuniform motion resampled into a uniform displacement axis, lateral motion artifacts are corrected. (d) Measured stage velocities of (a) and (b). Note that the high frequency oscillations are typical for lead screw translation stages.

velocity. The corresponding velocity profiles are shown in Fig. 1(d). It can be observed that the pitch of the ridge pattern decreases in areas where the scan velocity was relatively high and that it increases in areas of relatively low velocity. The computed displacement trajectory is used to resample the ensemble of A-lines from a uniform time axis into a uniform displacement axis, yielding a morphologically correct B-mode image of the phantom shown in Fig. 1(c).

The displacement error is characterized by scanning five times over 5953 μm of the phantom. The mean measured displacement is 5950 ± 6 μm, which is in good agreement with the 5.5 μm accuracy of the translation stage [6]. The error given by (2) for these scans is 0.6 μm with a measured $\Delta\phi = 1.6$ mrad, $N = 224200$, $\theta = 82.76°$, and $n = 1.363$.

A tissue phantom with homogeneously distributed stationary scatterers represents an idealized case. However, since the method relies on Doppler information available from discrete depths within the sample, it allows for the continuous acquisition of flow velocity profiles of moving particles and the simultaneous measurement of the lateral movement of the probe beam. To illustrate this, we measured the three-dimensional flow profile in a tissue phantom containing a flow channel in which a 1 vol. % Intralipid (Fresenius Kabi) solution was flowing. B-mode OCT images were acquired by translating the stage with quasi-uniform velocity across the flow channel. In this configuration, the total Doppler shift is a vectorial sum of the shift generated by the flowing particles and the shift produced by the moving stage. Figure 2(a) shows a segment of a B-scan of the tissue phantom with the flow channel. Figure 2(b) shows the lateral velocity profiles taken at two depths indicated with arrows. By accounting for the movement of the stage from depths close to the surface, the correct flow profile is reconstructed with zero flow velocity outside the flow channel.

As an application of the presented technique we performed a hand-held B-mode acquisition of *in vivo* skin of one of the author's ventral forearms. A spacer with a large glide surface was added to the sample arm to fix the distance between the objective lens and the surface of the skin and to maintain a constant angle during scanning. The raw and resampled OCT images are shown in Fig. 3. A clear reduction in the image artifacts can be observed after resampling the ensemble of A-lines with the corresponding displacement trajectory measured near the surface. The extent of the lateral displacement axis, calculated based on the Doppler shift, compares well with a direct measurement of the total displacement of 59 ± 5 mm.

During *in vivo* hand-held skin measurements, abrupt accelerations are observed which degraded the accuracy of the displacement measurement. We believe that these originate from the friction between the elastic skin and

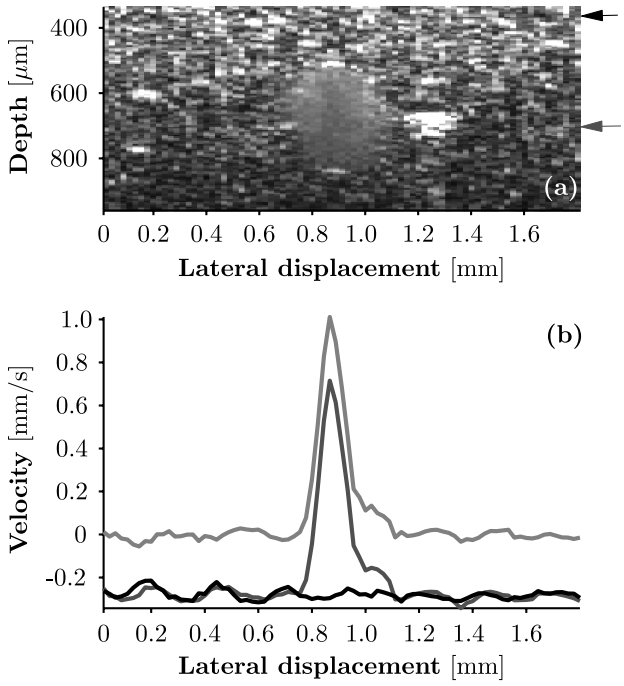

Fig. 2. (a) OCT image of the tissue phantom with a channel with flowing Intralipid solution. (b) Velocity while translating the stage, measured through the flow channel (dark gray line/arrow) and measured at a shallower depth (black line/arrow). The flow profile is calculated by subtracting both signals (light gray line).

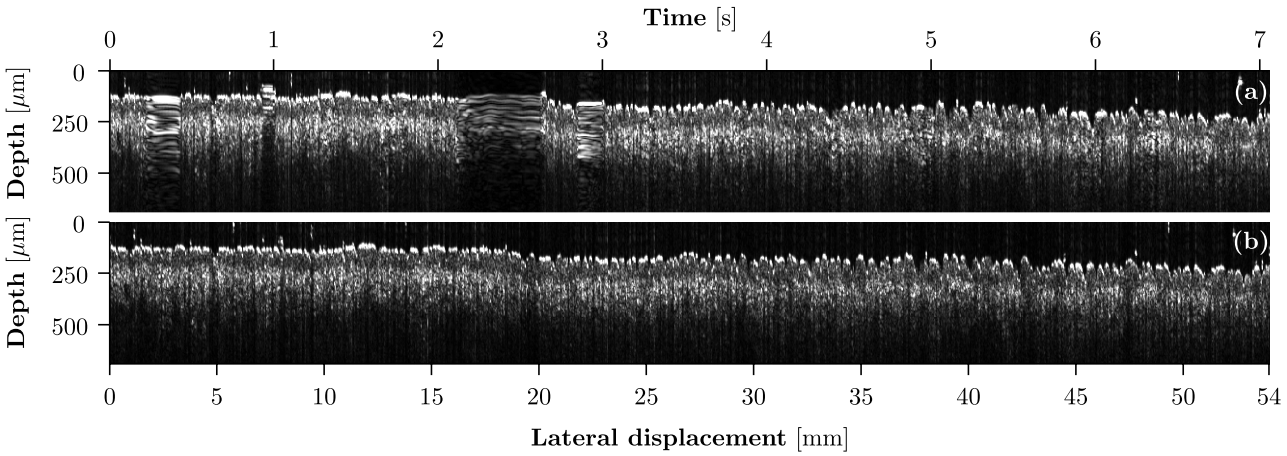

Fig. 3. Hand-held B-mode OCT image of the skin of the ventral forearm. (a) B-scan plotted in a uniform time axis. (b) B-scan resampled and plotted in a uniform displacement axis correcting for the lateral scanning artifacts caused by the nonuniform motion of the OCT probe.

the imaging probe. A solution to this problem is the use of refractive index matching media or ultrasound gel to reduce the friction at the probe–skin interface, which has the additional advantage to reduce OCT image artifacts, such as intensity distortions [7].

The method presented here is accurate and simple, but suffers from problems generally associated with integration-based estimation methods and with Doppler OCT, such as accumulation of errors, phase wrapping at high velocities [8], a decrease of lateral resolution, and a decrease of signal-to-noise ratio [9]. In general, these problems can be solved by using higher acquisition rates. More importantly, in the current implementation of the Doppler-based motion tracking only one component of the two-dimensional velocity vector in the plane of motion of the probe is measured. Nevertheless, as long as the orientation of the probe relative to the direction of motion and the angle θ in (1) remain constant during the image acquisition procedure, morphologically correct images are obtained. The full velocity vector can be obtained by combining the Doppler shift of two OCT beams or by determining the magnitude of the velocity vector using, e.g., decorrelation techniques [10]. Lastly, the assumption that the refractive index is constant at a fixed depth is not met for *in vivo* applications.

In conclusion, we demonstrated a simple method to accurately measure the displacement trajectory of a moving OCT probe based on the depth-resolved phase information. The experiments demonstrate that the nformation carried by the OCT signal fully suffices for the correction of images from nonuniform lateral scanning artifacts, as well as for continuous large scale B-mode acquisition of morphologically correct images and flow.

The authors thank D. M. de Bruin and M. Shehata for support. This work has been supported by the IOP Photonic Devices program managed by the Technology Foundation STW and Agentschap NL.

References

1. A. Ahmad, S. G. Adie, E. J. Chaney, U. Sharma, and S. A. Boppart, Opt. Express **17**, 8125 (2009).
2. J. Ren, J. Wu, E. J. McDowell, and C. Yang, Opt. Lett. **34**, 3400 (2009).
3. M. A. Choma, A. K. Ellerbee, S. Yazdanfar, and J. A. Izatt, J. Biomed. Opt. **11**, 024014 (2006).
4. J. Kalkman, A. V. Bykov, D. J. Faber, and T. G. van Leeuwen, Opt. Express **18**, 3883 (2010).
5. D. M. de Bruin, R. H. Bremmer, V. M. Kodach, R. de Kinkelder, J. van Marle, T. G. van Leeuwen, and D. J. Faber, J. Biomed. Opt. **15**, 025001 (2010).
6. Zaber Technologies, Zaber T-series positioning products technical notes (2006).
7. Y. M. Liew, R. A. McLaughlin, F. M. Wood, and D. D. Sampson, J. Biomed. Opt. **16**, 116018 (2011).
8. H. C. Hendargo, R. P. McNabb, A. Dhalla, N. Shepherd, and J. A. Izatt, Biomed. Opt. Express **2**, 2175 (2011).
9. S. H. Yun, G. J. Tearney, J. F. de Boer, and B. E. Bouma, Opt. Express **12**, 2977 (2004).
10. J. M. Rubin, T. A. Tuthill, and J. B. Fowlkes, Ultrasound Med. Biol. **27**, 101 (2001).